

WUE-ITP-97.045  
hep-ph/9712354

# Angular and Energy Distribution in Neutralino Production and Decay with complete Spin Correlations<sup>1</sup>

G. MOORTGAT-PICK<sup>2</sup>

*Institut für Theoretische Physik, Universität Würzburg, Am Hubland,  
D-97074 Würzburg, Germany*

H. FRAAS<sup>3</sup>

*Institut für Theoretische Physik, Universität Würzburg,  
D-97074 Würzburg, Germany*

## Abstract

We study the process  $e^-e^+ \rightarrow \tilde{\chi}_1^0\tilde{\chi}_2^0$  with the subsequent decay  $\tilde{\chi}_2^0 \rightarrow \tilde{\chi}_1^0\ell^+\ell^-$  taking into account the complete spin correlations between production and decay. We present numerical results for the lepton angular distribution and the distribution of the opening angle between the outgoing leptons for  $\sqrt{s} = 182$  GeV. We examine representative mixing scenarios in the MSSM and study the influence of the common scalar mass parameter  $m_0$ . For the lepton angular distribution the effect of the spin correlations amounts to up to 20%. The shape of the lepton angular distribution is very sensitive to the mixing in the gaugino sector and to the value of  $m_0$ . We find that the opening angle distribution is suitable for distinguishing between Higgsino-like and gaugino-like neutralinos.

---

<sup>1</sup> Work supported by the German Federal Ministry for Research and Technology (BMBF) under contract number 05 7WZ91P (0).

<sup>2</sup> e-mail: gudi@physik.uni-wuerzburg.de

<sup>3</sup> e-mail: fraas@physik.uni-wuerzburg.de

## 1. Introduction

The most economical candidate for a realistic SUSY model with minimal content of particles is the Minimal Supersymmetric Extension of the Standard Model (MSSM). Here the SUSY particles can only be produced in pairs and the lightest supersymmetric particle (LSP), usually assumed to be the lightest neutralino  $\tilde{\chi}_1^0$ , is stable and escapes detection.

Angular distributions and angular correlations of the decay products of neutralinos can give valuable information on their mixing character and are necessary for constraining the parameter space of the MSSM. Since decay angular distributions depend on the polarization of the parent particles one has to take into account spin correlations between production and decay.

## 2. General Formalism

Both the production process,  $e^-e^+ \rightarrow \tilde{\chi}_1^0\tilde{\chi}_2^0$ , and the decay process,  $\tilde{\chi}_2^0 \rightarrow \tilde{\chi}_1^0\ell^+\ell^-$  contain contributions from  $Z^0$  exchange in the direct channel and from  $\tilde{\ell}_L$  and  $\tilde{\ell}_R$  exchange in the crossed channels [1].

The helicity of the decaying neutralino  $\tilde{\chi}_2^0$  is denoted by  $\lambda_2$ . The amplitude  $T = \Delta_2 P^{\lambda_2} D_{\lambda_2}$  of the combined process is a sum over all polarization states of the helicity amplitude  $P^{\lambda_2}$  for the production process times the helicity amplitude  $D_{\lambda_2}$  for the decay process and a pseudopropagator  $\Delta_2 = 1/[s_2 - m_2^2 + im_2\Gamma_2]^{-1}$  of  $\tilde{\chi}_2^0$ . The effective mass squared of  $\tilde{\chi}_2^0$  is denoted by  $s_2$ , the mass by  $m_2$  and the width by  $\Gamma_2$ . The amplitude squared  $|T|^2 = |\Delta_2|^2 \rho_P^{\lambda_2\lambda_2'} \rho_{\lambda_2'\lambda_2}^D$  is thus composed from the unnormalized spin density matrix  $\rho_P^{\lambda_2\lambda_2'} = P^{\lambda_2} P^{\lambda_2'*}$  of  $\tilde{\chi}_2^0$  and the decay matrix  $\rho_{\lambda_2'\lambda_2}^D = D_{\lambda_2} D_{\lambda_2'}^*$  for the respective decay channel. All helicity indices but that of the decaying neutralino are suppressed. Repeated indices are summed over [2].

Interference terms between various helicity amplitudes preclude factorization in a production factor  $\sum_{\lambda_2} |P^{\lambda_2}|^2$  times a decay factor  $\sum_{\lambda_2} |D_{\lambda_2}|^2$  as for the case of spinless particles.

We split the phase space into that for production, and that for decay and obtain the differential cross section in the  $e^-e^+$ -cms by integrating over the effective mass squared  $s_2$  of  $\tilde{\chi}_2^0$ . Since the total width of  $\tilde{\chi}_2^0$  is much smaller than its mass ( $\Gamma_2 \ll m_2$ ) we make the narrow width approximation:  $\frac{1}{(s_2 - m_2^2)^2 + m_2^2\Gamma_2^2} \approx \frac{\pi}{m_2\Gamma_2} \delta(s_2 - m_2^2)$ .

## 3. Numerical Results and Discussion

Neutralinos are linear superpositions  $(\tilde{\gamma}|\tilde{Z}|\tilde{H}_a^0|\tilde{H}_b^0)$  of the photino  $\tilde{\gamma}$  and the zino  $\tilde{Z}$ , coupling to sleptons, and the two Higgsinos  $\tilde{H}_a^0$  and  $\tilde{H}_b^0$ , coupling to  $Z^0$ . The composition of the neutralino states depend on the three SUSY mass parameters  $M, M'$  ( with  $M' = \frac{5}{3}M \tan^2 \theta_W$  suggested by GUT [3]) and  $\mu$ , and on the ratio  $\tan \beta = v_2/v_1$  of the vacuum expectation values of the Higgs fields. We choose  $\tan \beta = 2$ . The masses of the sleptons are determined by  $M$  and  $\tan \beta$  and the common scalar mass parameter  $m_0$  [4]. We shall consider three representative scenarios which differ significantly in the nature of the two lowest mass eigenstates  $\tilde{\chi}_1^0$  and  $\tilde{\chi}_2^0$  ( (A)  $M=78$  GeV,  $\mu = -250$  GeV; (B)  $M=100$  GeV,  $\mu = 400$  GeV; (C)  $M=210$  GeV,  $\mu = -60$  GeV ) and two values of the scalar mass,  $m_0 = 80$  GeV and  $m_0 = 200$  GeV. In (A)  $\tilde{\chi}_1^0 = (+.94| -.32| -.08| -.07)$  has a dominating photino component and  $\tilde{\chi}_2^0 = (-.34| -.90| -.16| -.23)$  has a dominating zino component. In (B) both neutralinos,  $\tilde{\chi}_1^0 = (-.76| +.63| -.13| +.09)$  and  $\tilde{\chi}_2^0 = (+.65| +.73| -.18| -.10)$ , are nearly equal photino-zino mixtures. In (C) both neutralino states are dominated by strong Higgsino components,  $\tilde{\chi}_1^0 = (-.10| +.17| -.19| +.96)$  and  $\tilde{\chi}_2^0 = (+.06| -.31| +.92| +.24)$ .

The total cross section for the combined process is independent of the spin correlations [5]. For  $\sqrt{s} = 182$  GeV and  $m_0 = 80$  GeV ( $m_0 = 200$  GeV) we obtain in (A) 36.1 fb (11.1 fb), in (B) 15.4 fb (2.9 fb) and in (C) 57.1 fb (57.2 fb).

### 3.1. Lepton angular distributions

We calculate the distribution of the lepton angle between the incoming  $e^-$  and the outgoing lepton  $\ell^-$  in the laboratory system,  $d\sigma/d\cos \Theta_-$ , and compare our results with those obtained from the assumption of factorization of the differential cross section into production and decay (Figs. 1–4).

The spin effect is sizeable in the gaugino-like scenario (A). In the forward and backward direction it amounts to about 15% for  $m_0 = 80$  GeV and to more than 20% for  $m_0 = 200$  GeV (Fig. 1).

The magnitude of the resulting forward-backward (FB) asymmetry sensitively depends on the mixing-character of the neutralinos. In the gaugino-like scenario (B) for both values of  $m_0$  the contribution of spin correlations only amounts to at most 2.5% in the forward and backward direction. In the case of gaugino-like neutralinos the scalar mass  $m_0$  crucially determines the shape of the angular distributions. For  $m_0 = 80$  GeV it has a maximum nearly perpendicular to the beam direction and is almost FB symmetric (Fig. 2). For  $m_0 = 200$  GeV the shape has completely changed. It has a minimum in the backward hemisphere and the forward direction is favoured (Fig. 3).

In the Higgsino-like scenario (C) both production and decay are dominated by  $Z^0$ -exchange. Therefore the dependence on  $m_0$  is considerably smaller and we give only numerical results for  $m_0 = 80$  GeV. Here the contribution of spin correlations is negligible, maximally 0.3%, so that the angular distribution is practically FB-symmetric (Fig. 4).

### 3.2. The lepton opening angle distribution

The distribution of the opening angle between both outgoing leptons in the laboratory system,  $d\sigma/d\cos\Theta_{+-}$ , factorizes due to the Majorana character of the neutralinos.

The distributions are similar for both gaugino-like scenarios (A) and (B) (Figs. 5 and 6). In (B) they are symmetric with a maximum at  $\Theta_{+-} = \pi/2$  whilst for (A) larger angles between  $\pi/2$  and  $\pi$  are favoured.

For Higgsino-like neutralinos (Fig. 7), the shape is completely different from those of gaugino-like neutralinos. Here the lepton pairs are preferably emitted with small angles between them, approximately 60% of them with an opening angle between 0 and  $\pi/2$ .

The influence of varying the value of  $m_0$  is rather small; the shape remains essentially unchanged.

It is obvious that the distribution of the opening angle between the leptons is much more suitable for discrimination between gaugino- and Higgsino-like neutralinos than the lepton angular distribution.

### 3.3. Energy Distributions

In all three mixing scenarios the energy distribution of the outgoing lepton factorizes due to the Majorana character of the neutralinos.

The shapes of all scenarios are similar, therefore we only show the energy distribution of  $\ell^-$  for (A) for  $m_0 = 80$  GeV and  $m_0 = 200$  GeV (Fig. 8). The maximum is independent of the actual value of  $m_0$ . For more details see [6]. As a consequence of CP invariance and the Majorana character the energy spectra of both leptons,  $\ell^-$  and  $\ell^+$ , are identical [7].

## 4. Summary

In this paper we have considered the associated production of neutralinos,  $e^- + e^+ \rightarrow \tilde{\chi}_1^0 + \tilde{\chi}_2^0$ , and the subsequent direct leptonic decay,  $\tilde{\chi}_2^0 \rightarrow \tilde{\chi}_1^0 + \ell^+ + \ell^-$ , with complete spin correlations between production and

decay. The quantum mechanical interference terms between the various polarization states of the decaying neutralino give rise to a strong effect in the lepton angular distribution, whereas the opening angle distribution and the energy distribution are independent from these spin correlations.

The opening angle distribution turns out to be suitable for distinguishing between Higgsino-like and gaugino-like neutralinos. However, it is rather indifferent to variable mixing in the gaugino sector. The shape of the opening angle distribution only slightly depends on the scalar mass  $m_0$ . The lepton angular distribution, on the other hand, is not only very sensitive to the mixing in the gaugino sector but also to the actual value of  $m_0$ .

G. M.-P. thanks K. Kołodziej and the other organizers of the Ustron School for the friendly atmosphere during the Conference and the excellent organization. We thank A. Bartl and W. Majerotto for many useful discussions. We are grateful to V. Latussek for his support in the development of the numerical program.

#### REFERENCES:

- [1] A. Bartl, H. Fraas, W. Majerotto, Nucl.Phys. **B 278**, 1 (1986).
- [2] H.E. Haber, in Proceedings of the 21st SLAC Summer Institute on Particle Physics, Stanford 1993.
- [3] H.E. Haber, G.L. Kane, Phys. Rep. **117**, 75 (1985).
- [4] L.J. Hall, J. Polchinski, Phys. Lett. **B 152**, 335 (1985).
- [5] D.A. Dicus, E.C.G. Sudarshan, X. Tata, Phys. Lett. **B 154**, 79 (1985).
- [6] G. Moortgat-Pick, H. Fraas, hep-ph 9708481, for publ. in Phys.Rev.**D**.
- [7] S.T. Petcov, Phys. Lett **B139**, 421 (1984).

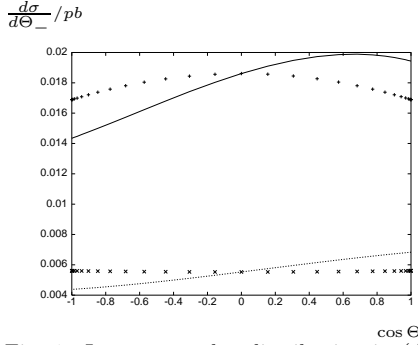


Fig. 1: Lepton angular distribution in (A) for  $m_0 = 80$  GeV with spin correlations fully taken into account (upper solid) and for assumed factorization (upper dotted); for  $m_0 = 200$  GeV with spin correlations (lower solid) and for assumed factorization (lower dotted).

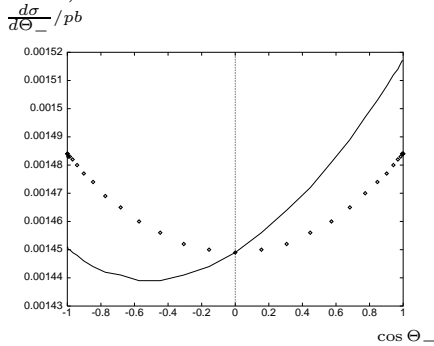


Fig. 3: Lepton angular distribution in (B) for  $m_0 = 200$  GeV with spin correlations fully taken into account (solid) and for assumed factorization (dotted).

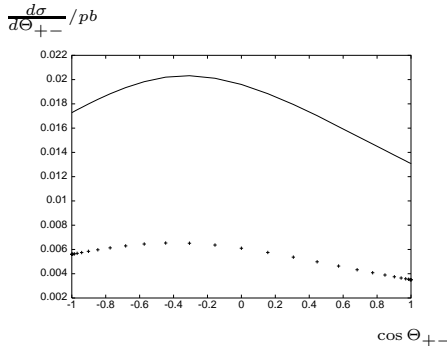


Fig. 5: Opening angle distribution in (A) for  $m_0 = 80$  GeV with spin correlations fully taken into account (solid); for  $m_0 = 200$  GeV with spin correlations (dotted).

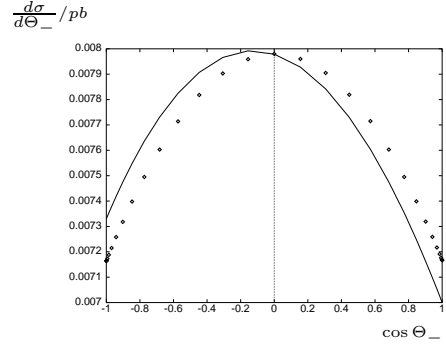


Fig. 2: Lepton angular distribution in (B) for  $m_0 = 80$  GeV with spin correlations fully taken into account (solid) and for assumed factorization (dotted).

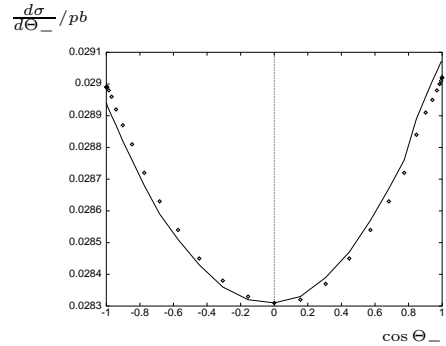


Fig. 4: Lepton angular distribution in (C) for  $m_0 = 80$  GeV with spin correlations fully taken into account (solid) and for assumed factorization (dotted).

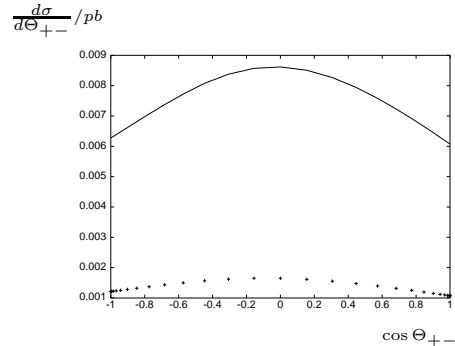


Fig. 6: Opening angle distribution in (B) for  $m_0 = 80$  GeV with spin correlations fully taken into account (solid); for  $m_0 = 200$  GeV with spin correlations (dotted).

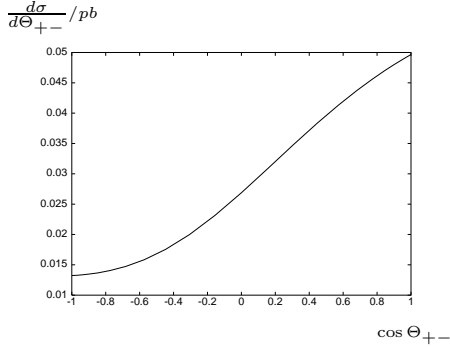


Fig. 7: Opening angle distribution in (C) for  $m_0 = 80$  GeV with spin correlations fully taken into account.

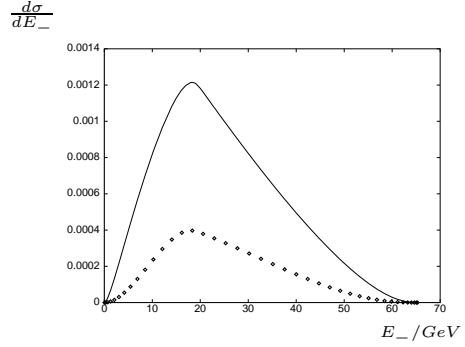


Fig. 8: Energy distribution in (A) for  $m_0 = 80$  GeV (solid) and for  $m_0 = 200$  GeV (dotted).